

PROTOPLANETARY DISK MASS DISTRIBUTION IN YOUNG BINARIES

ERIC L. N. JENSEN

Swarthmore College Department of Physics and Astronomy, Swarthmore, PA 19081 USA
ejensen1@swarthmore.edu

RACHEL L. AKESON

Interferometry Science Center, Caltech, MS 100-22, 1201 E. California Blvd., Pasadena, CA 91125 USA
rla@ipac.caltech.edu

Received 2002 September 4; accepted 2002 October 21

ABSTRACT

We present millimeter-wave continuum images of four wide (separations 210–800 AU) young stellar binary systems in the Taurus–Auriga star-forming region. For all four sources, the resolution of our observations is sufficient to determine the mm emission from each of the components. In all four systems, the primary star’s disk has stronger millimeter emission than the secondary and in three of the four, the secondary is undetected; this is consistent with predictions of recent models of binary formation by fragmentation. The primaries’ circumstellar disk masses inferred from these observations are comparable to those found for young single stars, confirming that the presence of a wide binary companion does not prevent the formation of a protoplanetary disk. Some of the secondaries show signatures of accretion ($H\alpha$ emission and $K-L$ excesses), yet their mm fluxes suggest that very little disk mass is present.

Subject headings: stars: formation, stars: pre-main sequence, circumstellar matter, binaries: general, planetary systems: formation, planetary systems: protoplanetary disks

1. INTRODUCTION

The majority of stars are in binary or multiple systems during both the pre–main–sequence and main–sequence phases of stellar evolution (see, e.g., reviews by Mathieu 1994; Mathieu et al. 2000). Therefore, understanding the causes and effects of multiplicity is an essential ingredient of complete models of both star and planet formation. Circumstellar disks play a crucial role in both processes by providing conduits for material to accrete onto the stars, and by providing sites for planet formation.

Only in the last few years have observations of young binaries and theories of binary formation both advanced to the point where direct comparison of observations and theory is possible. While such comparisons still cannot definitively establish the mechanism(s) of binary formation (e.g., Clarke 2001), increasingly there are opportunities to test predictions of binary formation models with observational data. Current observations are consistent with the formation of most low-mass binary systems by scale-free fragmentation of a molecular cloud (Clarke 2001; Ghez 2001). One notable prediction of such models is that the more massive star in the binary should always harbor the more massive circumstellar disk (Bate 2000).

We set out to test this prediction with the observations presented here. Previous work has shown that primary stars in young binary systems have more active (and thus perhaps more massive) disks than secondaries do. Primaries tend to have stronger signatures of the presence of circumstellar disks (red $K-L$ colors) and of accretion from such disks (strong $H\alpha$ and $Br\gamma$ emission) than secondaries do (Prato & Simon 1997; Duchêne et al. 1999; White & Ghez 2001; Prato & Monin 2001). However, such observations reflect the disk conditions near the stellar surfaces, where accretion takes place and where the vast majority of the near-infrared flux is produced. These observations suggest a dependence of disk properties on stellar mass in binaries, but in general these diagnostics (especially $H\alpha$ equivalent width) are at most only marginally correlated

with disk mass (Beckwith et al. 1990; Osterloh & Beckwith 1995). Thus, the optical and near-IR observations do not directly address the question of total disk masses in these systems, making comparison with theoretical predictions problematic. A measurement of the disk masses with millimeter interferometry is necessary for direct comparison with theoretical predictions. The work we present here has the advantages that we (a) observed circumstellar disks at a wavelength ($\lambda = 1.3$ mm) where they are likely to be optically thin, to probe their total masses; (b) resolved both components in the binaries; and (c) observed systems with mm fluxes that are typical of average T Tauri stars, not anomalously large.

A few binaries have been previously observed with millimeter interferometers, but the interpretation of their disk masses and morphologies is complicated by the presence of unresolved additional pairs in triple or quadruple systems (e.g., T Tau, Akeson, Koerner, & Jensen 1998; UZ Tau, Jensen, Koerner & Mathieu 1996). Also, some of these observations have resolved the circumbinary disks, but not the binary itself (GG Tau, Koerner, Sargent, & Beckwith 1993; Guilloteau, Dutrey, & Simon 1999; UY Aur, Duvert et al. 1998). Thus, these observations do not reveal the distribution of disk mass between the two stars in each system. The observations we report here avoid the complication of unresolved additional components (as far as we know, except in the case of UX Tau B) and thus allow us to determine the disk mass distribution in the circumstellar disks of four young binary systems.

We present our observations in Section 2 below. We then discuss the disk properties implied by our observations and other data (Sec. 3) and the implications of these results for our understanding of binary star formation and the prospects for planet formation in binary systems (Sec. 4).

2. OBSERVATIONS

We selected our targets from among known pre–main–sequence binaries in Taurus–Auriga based on the following cri-

teria: separation greater than $1''.1$, wide enough to resolve with the Owens Valley Millimeter Array (which has a resolution of $1''.1 \times 0''.8$ for a full track in the high-resolution configuration); and $\lambda = 1.3$ mm detection in the surveys of Beckwith et al. (1990) or Osterloh & Beckwith (1995). We did not restrict our sample to the brightest 1.3 mm sources, as limited sensitivity has necessitated in the past. We avoided triple and quadruple systems in which the closer pair(s) would be unresolved in our OVRO observations, since the presence of a companion with separation less than 100 AU is well-correlated with decreased millimeter emission (Beckwith et al. 1990; Osterloh & Beckwith 1995; Jensen, Mathieu, & Fuller 1996). We included UX Tau in our sample since the A, B, and C components can be resolved by OVRO; we did not realize until later that UX Tau B is itself a close binary. Our sample consists of three binary systems (DK Tau, HK Tau, and V710 Tau) and one quadruple system (UX Tau); source properties are summarized in Table 1. We note that the single-dish mm fluxes of these systems (35–73 mJy) are fairly typical of T Tauri star fluxes; the median flux among single stars in the samples of Osterloh & Beckwith (1995) and Beckwith et al. (1990) (including non-detections) is 36 mJy, while the median flux among binary stars is somewhat lower.

We observed the four systems in Table 1 with the Owens Valley millimeter-wave array on 11 and 19 January and 10 February 2002. We obtained data in both the low-resolution array (baselines 36–115 m; hour angle range ± 3 hours) and in the high-resolution array (baselines 35–240 m; hour angle range 0–3 hours). The correlator was configured with two wide-band channels centered around 230 GHz, and narrow band channels centered around $^{13}\text{CO}(2\rightarrow 1)$. The combination of both sidebands resulted in a total continuum bandwidth of 4 GHz.

During each observation, the array pointing was cycled among the four sources to provide similar hour angle coverage for each. The quasar J0449+135 was used as the gain calibrator and 3c454.3 and 3c273 were observed for use as flux calibrators. As our observations contained no measurements of primary flux calibrators (e.g., planets), we estimate the absolute flux calibration uncertainty to be 20%; relative fluxes are unaffected by this uncertainty. This uncertainty is based on the scatter in other measurements of 3c454.3 and 3c273 at OVRO that were calibrated using primary flux calibrators. The gain and flux calibrations were applied in the OVRO mma package. Maps were constructed and CLEANed in the MIRIAD package using a robust weighting which resulted in a $1''.5$ by $1''.3$ beam.

All four targets show at least one clearly-detected mm continuum source (Table 2; Figure 1). However, CO emission was not detected toward any of these sources; 3σ limits are 0.7–0.8 Jy, $T_{\text{antenna}} = 2.2\text{--}2.7$ K at a resolution of 0.33 km/s; or 0.3–0.4 Jy, $T_{\text{antenna}} = 1.0\text{--}1.3$ K when the spectra are binned to a resolution of 2 km/s. As discussed at the end of this section, our observations are less sensitive to emission on scales $> 5''$.

Three of the four systems show only one detected mm source. To determine which star is the source of the mm continuum emission, we overlaid the mm maps onto archival Hubble Space Telescope (HST) optical images of our sources taken in the F814W filter (similar to Cousins I). The absolute pointing accuracy of our observations is $0''.1$ as measured by quasar observations, but uncertainties in positions of the guide stars typically limit the accuracy of the HST/WFPC2 coordinates to $0''.7$ RMS (Baggett et al. 2002). Thus, to set the absolute coordinates in the HST images more accurately we used coordinates

for our targets from the Hipparcos catalog (for UX Tau only) or from the USNO A2.0 catalog (Monet et al. 1998). We used proper motions from Hipparcos or Jones & Herbig (1979) to transform these coordinates to the epoch of the OVRO observations. Since the USNO A2.0 coordinates do not resolve the binary systems, we assigned these coordinates to the photocenter of the emission measured in the HST images. The results are shown in Figure 1. In all cases, the source of the mm emission is unambiguous, since it aligns with the optical emission of a star to within $0''.1\text{--}0''.2$. In each case, the stronger mm emission comes from the primary star, and in three of the four systems the secondary is undetected.

All of the mm detections except for UX Tau A are unresolved point sources. UX Tau A is marginally resolved; an elliptical Gaussian fit to the millimeter emission gives a FWHM size of $1''.1 \times 0''.6$. As this is at the limit of our resolution, the exact size is uncertain; however, the clear difference between the source’s integrated flux and peak flux indicates that it is definitely resolved. The components of HK Tau A and B are consistent with unresolved point sources, but there is some additional diffuse emission between the two.

As can be seen in Table 2, our fluxes appear to be somewhat lower than the single-dish 1.3 mm fluxes for these sources. There are two possible explanations for this. One is that there is a systematic offset in the absolute flux calibration of the two datasets. As noted above, our absolute calibration is uncertain by 20%; Beckwith et al. (1990) and Osterloh & Beckwith (1995) use different calibration sources than we do and also cite a 20% flux calibration uncertainty. If we increase our fluxes by 20% and take into account the random uncertainties of each observation, then all of our measurements are still less than the single-dish fluxes, differing by 1.8, 0.9, 0.06, and 2.7σ for DK Tau, HK Tau, UX Tau, and V710 Tau respectively. If we shift our data up by 20% and the single-dish fluxes down by 20%, then the differences are 0.8, -0.4 , -1.1 , and 1.6σ , with half of our measurements now being slightly higher than the single-dish fluxes.

Alternatively, if the flux calibrations are correct, then the discrepancy could be explained by the fact that the interferometric measurements are not sensitive to extended emission. Although a discrepancy between interferometric and single-dish flux measurements is expected for younger sources from which there is substantial envelope emission, T Tauri sources are expected to have little if any envelope component (see, e.g., HL Tau vs. L1551 IRS 5 in Lay et al. 1994). The percentage of the single-dish flux detected for our sources ranges from 46 to 83%. Given the uv coverage of our observations, emission must have a size scale greater than $5''$ before half of the emission is filtered out in the interferometric data.

Prato & Simon (1997) have suggested that an extended circumprimary envelope could replenish the disks in T Tauri binary systems, though it is unclear how these envelopes could persist for so long (e.g., Clarke 2001). While our observations could be taken as support for existence of such an extended component, we caution that further observations are necessary to resolve the flux calibration issue.

3. DISK PROPERTIES

In this section, we attempt to determine the properties of the circumprimary and circumsecondary disks in our target systems. We first discuss what can be determined about the disks from existing optical and infrared data, and then we address the

disk properties as revealed by our new observations.

3.1. *Disk properties inferred from optical and infrared data*

Resolved spectra of the individual stars in our target binaries are presented in Cohen & Kuhl (1979); Magazzu, Martín, & Rebolo (1991); Hartigan, Strom, & Strom (1994); Monin, Ménard, & Duchêne (1998), and Duchêne et al. (1999). We have quoted the range of literature spectral types in Table 1. We adopted the spectral types given by Duchêne et al. (1999) for all systems except V710 Tau, for which we used the spectral types from Hartigan, Strom, & Strom (1994). In most cases, the different references agree fairly well about the spectral types; however, two cases merit some discussion. For DK Tau, Hartigan, Strom, & Strom (1994) list spectral types of K7 for both components, raising the question of whether it is clear which star is the primary. While Hartigan, Strom, & Strom (1994) do not show their spectra of DK Tau, the spectra shown in Monin, Ménard, & Duchêne (1998) clearly show DK Tau B (their label) to be later in spectral type than DK Tau A. Second, optical and infrared photometry in the literature consistently show DK Tau A to be the brighter star. Thus, the choice of primary in this system seems clear.

In HK Tau, on the other hand, the spectra shown by Monin, Ménard, & Duchêne (1998) appear to be quite similar in spectral type. We adopt the M2 and M3 classifications of Duchêne et al. (1999), which are based on the Monin, Ménard, & Duchêne (1998) spectra, but we note that the two stars are extremely close in spectral type. HK Tau B is much fainter, but most (if not all) of this difference is due to its edge-on disk blocking the direct starlight (Stapelfeldt et al. 1998; Koresko 1998).

The papers cited in the previous two paragraphs also present some resolved photometry, as do White & Ghez (2001) (K and L for all sources), Moneti & Zinnecker (1991) (JHK for UX Tau), Koresko (1998) (JHK for HK Tau), and Stapelfeldt et al. (1998) (JHK , F606W, and F814W [HST filters similar to V and I] for HK Tau).

All of these systems were detected by IRAS and thus have substantial mid- and far-infrared emission. However, the IRAS observations do not resolve the binaries and thus it is unclear which of the binary components is the source of the infrared excess. Indeed, prior to the observations reported here, none of these systems had been resolved at a wavelength longer than $3.6 \mu\text{m}$ (L band).

With the available *resolved* optical and infrared data, then, the best tracers of the presence of circumstellar material are $H\alpha$ emission (presumed to arise from accretion onto the stellar surfaces) and $K-L$ color (which can reveal the presence of an infrared excess indicative of a disk). These quantities are given in Table 1.

Among optical and near-infrared colors, $K-L$ is well-suited for tracing circumstellar material because it is relatively unaffected by interstellar reddening, and because the photospheric colors of late-type stars have a relatively small range of values, minimizing the effect of uncertainties in spectral typing on the calculation of a color excess (White & Ghez 2001). To determine the $K-L$ color excesses $\Delta(K-L)$ given in Table 1, we used the photospheric colors of Bessell & Brett (1988), which range from 0.10–0.20 for the range of spectral types in our sample.

Both the $H\alpha$ emission and $\Delta(K-L)$ in Table 1 tell the same story. Stars classified as classical T Tauri Stars (CTTS) based

on $H\alpha$ equivalent width ($\geq 5 \text{ \AA}$ for K stars, $\geq 10 \text{ \AA}$ for early M stars; see Martín 1997) also have significant ($> 2.5-3\sigma$) $\Delta(K-L)$ color excesses. The borderline CTTS V710 Tau B has only a borderline $\Delta(K-L)$ excess as well. All four systems thus have primary stars with evidence for disks. DK Tau and HK Tau also have secondaries with evidence for disks, while V710 B is marginal, and UX Tau B and C show little evidence of disk material.

3.2. *Disk properties inferred from millimeter observations*

As noted above, the most striking thing about the observed millimeter fluxes from these systems is the how completely the primary stars dominate the systems' mm emission.

3.2.1. *Comparison with optical and infrared disk properties*

There is not a one-to-one correlation between the properties discussed in the preceding section and the millimeter fluxes in our observations (Figure 2). While it appears that strong $H\alpha$ emission and $K-L$ excess are necessary conditions for the presence of a millimeter detection, they are clearly not sufficient, since DK Tau B shows strong $\Delta(K-L)$ and $H\alpha$, but no millimeter emission. This is most likely due to the fact that the optical and near-infrared emission arise in a relatively small region of the disk close to the star, while the mm flux is more broadly distributed. Thus, each diagnostic has its advantages. $H\alpha$ emission and $K-L$ excess can be sensitive to relatively small disks that are undetected at millimeter wavelengths, while mm emission is a better tracer of global disk properties, especially disk mass. Disk mass is the property that is crucial for testing binary formation models, and it is there that we now turn our attention.

3.2.2. *Disk mass estimates*

Millimeter-wavelength observations have often been used in conjunction with optical and infrared data to model the spectral energy distributions of T Tauri stars, with the optical and infrared data providing some constraint on the disk temperature distribution, and the millimeter data providing a tracer of optically thin material in order to determine the disk mass (e.g., Beckwith et al. 1990; Osterloh & Beckwith 1995). However, there is not enough resolved mid- and far-infrared data available for these binaries to justify detailed modeling of their spectral energy distributions.

Limits on the disk masses can be estimated by assuming that all emission is from optically-thin material with a given temperature. These estimated disk masses (Table 3) are a lower limit to the true disk mass. We use the canonical value for the dust emissivity κ_ν from Hildebrand (1983) of $0.1 \text{ cm}^2 \text{ g}^{-1}$ at $\lambda = 250 \mu\text{m}$ with a frequency scaling $\kappa_\nu \propto \nu^\beta$ of $\beta = 1$.

The assumption that the disks are entirely optically thin at 1.3 mm is unlikely to be correct for the primary stars with detected 1.3 mm flux, and so these masses are lower limits to the true disk mass. However, we note that these mass estimates are comparable to those obtained from detailed models (Beckwith et al. 1990; Osterloh & Beckwith 1995) of stars with similar mm fluxes, suggesting that the optically-thin approximation may be reasonably good. In their T Tauri disk survey at $\lambda = 2.7 \text{ mm}$, Dutrey et al. (1996) estimated that optically thick emission accounted for $\lesssim 10\%$ of the total mass for 13 of 15 sources. Using their assumed disk model to extend these results to $\lambda = 1.3 \text{ mm}$, optically thick emission at $\lambda = 1.3 \text{ mm}$ accounts for less than 20% of the total mass in 13 of 15 sources.

3.2.3. Disk size estimates

Alternatively, if we assume that the millimeter flux comes entirely from optically *thick* material, we can estimate the minimum size of the emitting region. If a disk inclination value is assumed (we used $\cos i = 0.5$) and the temperature is described as a power law function of radius, $T(r) = T(r_0) * (r/r_0)^{-q}$, then for a given flux, the outer radius for a completely optically thick disk depends only on $T(r_0)$ and q . For each source, we calculated the outer radius using $T(r_0) = 150$ K and $q = 0.5$. The calculated radii are given in Table 3. Calculations using the $T(r_0)$ and q values derived for each source in Beckwith et al. (1990) yielded similar results. These radii can be interpreted as lower limits to the true disk radii, since it is likely that some of the emission is optically thin. The derived radii are similar to the limits found by Dutrey et al. (1996) for circumstellar disks around single T Tauri stars.

4. DISCUSSION

The 1.3 mm flux in these systems is clearly dominated by the primary star. The essential question for comparison of these observations with predictions of theories of binary formation is whether or not this larger flux indicates a larger disk mass around the primaries as well.

While some of the observed flux difference may be attributable to the primaries' disks being hotter, we argue that the primaries must in fact have more massive disks than the secondaries. The primary and secondary stellar effective temperatures differ by less than 10% in three of the four systems, and by 22–28% in UX Tau. A temperature difference of this magnitude is not sufficient to account for the observed flux difference if the disks have similar masses and opacities.

Another argument that could be made against the higher mm fluxes resulting from higher-mass disks is that the disk inclinations of the secondaries might be different from those of the primaries, with the primaries presenting a larger projected surface area and thus a larger mm flux from (perhaps) a similar disk mass. The problem with this hypothesis is that it requires a coincidence, namely that secondaries happen to be more edge-on to Earth than the primaries in all four cases. Another problem arises in the case of HK Tau, where the inclination of the secondary disk is known to be fairly edge-on to Earth (roughly 5° ; Stapelfeldt et al. 1998) and the primary and secondary disks are clearly not coplanar. This is the system that has perhaps the most edge-on secondary disk, yet it is the only system in our sample in which the secondary was detected. This argues strongly against all the secondary disks being undetected due to an edge-on geometry. For equal-mass optically-thin primary and secondary disks, only extreme inclination angles for the secondaries would result in the primary/secondary flux ratios measured here. Inclination angles this extreme would probably obscure the optical emission from the secondary, which is only the case for HK Tau (Figure 1). Finally, Jensen, Donar, & Mathieu (2000) find that among wide binaries in general, primary and secondary disks tend to be aligned with each other to within $\sim 20^\circ$, making it unlikely that we would see significant flux differences due to inclination differences alone.

Thus, the secondaries not only have lower millimeter fluxes, but they almost certainly have lower-mass disks. This is in excellent agreement with binary formation models of scale-free fragmentation (e.g., Bate 2000; Clarke 2001).

Examining the relationship between stellar mass and disk mass suggests that the disk properties we observe are some-

how related to the dynamics of binary formation and evolution, and not just to the mass of each individual star. Some of the secondary stars in the systems discussed here are roughly equal in mass to some of the primaries; for example, HK Tau A and DK Tau B are both spectral type M1, and therefore are very close in mass; V710 Tau A is also close at spectral type M0.5. Despite this similarity, HK Tau A and V710 Tau A, the more massive stars in their respective systems, have detectable mm flux (and therefore more massive disks) while DK Tau B has a very small mm flux, below our sensitivity limit (Figure 3). While our sample is small and thus we cannot draw definitive conclusions about all young binaries, our data suggest that it is not the individual stellar masses in a binary system that determine the distribution of disk mass within the system. Rather, the primary (regardless of its absolute mass) retains a more substantial disk. In this scenario, the fact that both components in HK Tau have detectable disks is consistent with the fact that it is the only system in which the primary and secondary spectral types are virtually indistinguishable.

It is also notable that the disk masses derived for the primaries are similar to those derived for single T Tauri stars by Beckwith et al. (1990) and Osterloh & Beckwith (1995), especially considering that our mass estimates are lower limits. This suggests that a wide (> 200 AU) binary companion does not prevent the formation of a circumstellar disk that is near the mass of the minimum mass solar nebula, consistent with the conclusions of Jensen, Mathieu, & Fuller (1996). In fact, this result strengthens the prospects for planet formation in wide binaries, since it suggests that most of the disk mass in these systems resides in a single, more massive disk rather than two smaller disks, thus providing a larger reservoir of material for planet formation around the primary.

The upper limits on the mm flux from the secondaries do not, in and of themselves, set these stars apart from single stars; roughly half of the single stars in the sample of Osterloh & Beckwith (1995) were not detected at 1.3 mm. What is striking, as emphasized before, is the comparison between the mm emission of the primary and that of the secondary. This is especially notable since a comparison of primary and secondary disks within a given binary system is effectively controlled for the effects of age and formation environment. These factors allow for the persistence of a substantial disk around the primaries in our sample, and yet most of the secondaries are relatively devoid of disk material.

Several studies (see, e.g., the review by Prato & Monin 2001) have shown that T Tauri binaries tend to occur in matched pairs, i.e. it is much more common to find classical T Tauri stars (CTTS) paired with other CTTS and weak-lined T Tauri stars (WTTS) paired with other WTTS than it is to find mixed CTTS/WTTS pairs. The fact that both stars in a system are CTTS does not mean that their disks are similar, however. While $H\alpha$ traces disk accretion, it is not a good tracer of disk mass (e.g., Beckwith et al. 1990). Our results here reinforce the disparity between accretion diagnostics and disk mass: while most of the secondaries are CTTS, they have very low-mass disks (Table 3) and thus their disks are fairly different from those around the primaries. The most notable example is DK Tau B, with an $H\alpha$ emission equivalent width of 118 \AA but no detectable $\lambda = 1.3$ mm emission. Thus, while both primary and secondary in a binary system are often CTTS, primaries and secondaries can have very different disk masses.

5. CONCLUSIONS

We have presented $\lambda = 1.3$ mm continuum images of four young binary systems, showing that the primary star has a more massive disk in all cases; this is consistent with leading models of binary formation by fragmentation. These circumprimary disks are comparable in mass to those found around single T Tauri stars, indicating that the presence of a wide binary formation does not prevent the formation and survival of a disk massive enough to form a solar system like our own. In some systems, the secondary star shows evidence of strong accretion, but no detectable mm emission, indicating that the reservoir of accreting material has a relatively low mass. None of the sys-

tems observed has detectable $^{13}\text{CO}(2\rightarrow 1)$ emission at the sensitivity limit of our observations.

This work was performed in part at the Interferometry Science Center, California Institute of Technology. The Owens Valley millimeter-wave array is supported by NSF grant AST 96-13717. ELNJ gratefully acknowledges the support of the National Science Foundation's Life in Extreme Environments program through grant AST 99-96278, and Swarthmore College through a James Michener Fellowship. We thank the anonymous referee, whose detailed comments improved the presentation of this work. We thank Rabi Whitaker for a careful reading of the paper.

REFERENCES

- Akeson, R. L., Koerner, D. W., & Jensen, E. L. N. 1998, *ApJ*, 505, 358
 Allen, C. W., 1991, *Astrophysical Quantities*, 3rd edition (London: The Athlone Press)
 Baggett, S., et al. 2002, *HST WFPC2 Data Handbook*, v.4.0, ed. B. Mobasher (Baltimore: STScI), Sec. 5.4
 Baraffe, I., Chabrier, G., Allard, F., & Hauschildt, P. H. 1998, *A&A*, 337, 403
 Bate, M. R. 2000, *MNRAS*, 314, 33
 Beckwith, S. V. W., Sargent, A. I., Chini, R. S., & Güsten, R. 1990, *AJ*, 99, 924 (BSCG)
 Bessell, M. S. & Brett, J. M. 1988, *PASP*, 100, 1134
 Clarke, C. J. 2001, in *Birth and Evolution of Binary Stars*, Proceedings of IAU Symposium 200, 346
 Cohen, M. & Kuhl, L. V. 1979, *ApJS*, 41, 743
 Duchêne, G., Monin, J.-L., Bouvier, J., & Ménard, F. 1999, *A&A*, 351, 954
 Dutrey, A., Guilloteau, S., Duvert, G., Prato, L., Simon, M., Schuster, K., & Ménard, F. 1996, *A&A*, 309, 493
 Duvert, G., Dutrey, A., Guilloteau, S., Menard, F., Schuster, K., Prato, L., & Simon, M. 1998, *A&A*, 332, 867
 Ghez, A. M. 2001, in *Birth and Evolution of Binary Stars*, Proceedings of IAU Symposium 200, 210
 Guilloteau, S., Dutrey, A., & Simon, M. 1999, *A&A*, 348, 570
 Hartigan, P., Strom, K. M., & Strom, S. E. 1994, *ApJ*, 427, 961
 Hildebrand, R. H. 1983, *QJRAS*, 24, 267
 Jensen, E. L. N., Donar, A. X., & Mathieu, R. D. 2000, in *Birth and Evolution of Binary Stars*, Poster Proceedings of IAU Symposium 200, 85P
 Jensen, E. L. N., Mathieu, R. D. & Fuller, G. A. 1996, *ApJ*, 458, 312
 Jensen, E. L. N., Koerner, D. W. & Mathieu, R. D. 1996, *AJ*, 111, 2431
 Jones, B. F. & Herbig, G. H. 1979, *AJ*, 84, 1872
 Koerner, D. W., Sargent, A. I., & Beckwith, S. V. W. 1993, *ApJ*, 408, L93
 Koresko, C. D. 1998, *ApJ*, 507, L145
 Lay, O. P., Carlstrom, J. E., Hills, R. E., & Phillips, T. G. 1994, *ApJ*, 434, L75
 Leinert, C., Zinnecker, H., Weitzel, N., Christou, J., Ridgway, S. T., Jameson, R., Haas, M., & Lenzen, R. 1993, *A&A*, 278, 129
 Luhman, K. L. 1999, *ApJ*, 525, 466
 Luhman, K. L. 2000, *ApJ*, 544, 1044
 Magazzu, A., Martín, E. L., & Rebolo, R. 1991, *A&A*, 249, 149
 Martín, E. L. 1997, *A&A*, 321, 492
 Mathieu, R. D. 1994, *ARA&A*, 32, 465
 Mathieu, R. D., Ghez, A. M., Jensen, E. L. N. & Simon, M. 2000, *Protostars and Planets IV* (Tucson: University of Arizona Press; eds Mannings, V., Boss, A. P., Russell, S. S.), p. 703
 Monet, D., Bird, A., Canzian, B., Dahn, C., Guetter, H., Harris, H., Henden, A., Levine, S., Luginbuhl, C., Monet, A. K. B., Rhodes, A., Riepe, B., Sell, S., Stone, R., Vrba, F., & Walker, R., *The USNO-A2.0 Catalogue*, (Washington DC: U.S. Naval Observatory)
 Moneti, A. & Zinnecker, H. 1991, *A&A*, 242, 428
 Monin, J.-L., Ménard, F., & Duchêne, G. 1998, *A&A*, 339, 113
 Osterloh, M. & Beckwith, S. V. W. 1995, *ApJ*, 439, 288
 Prato, L. & Monin, J. 2001, in *Birth and Evolution of Binary Stars*, Proceedings of IAU Symposium 200, 313
 Prato, L. & Simon, M. 1997, *ApJ*, 474, 455
 Stapelfeldt, K. R., Krist, J. E., Menard, F., Bouvier, J., Padgett, D. L., & Burrows, C. J. 1998, *ApJ*, 502, L65
 White, R. J. & Ghez, A. M. 2001, *ApJ*, 556, 265

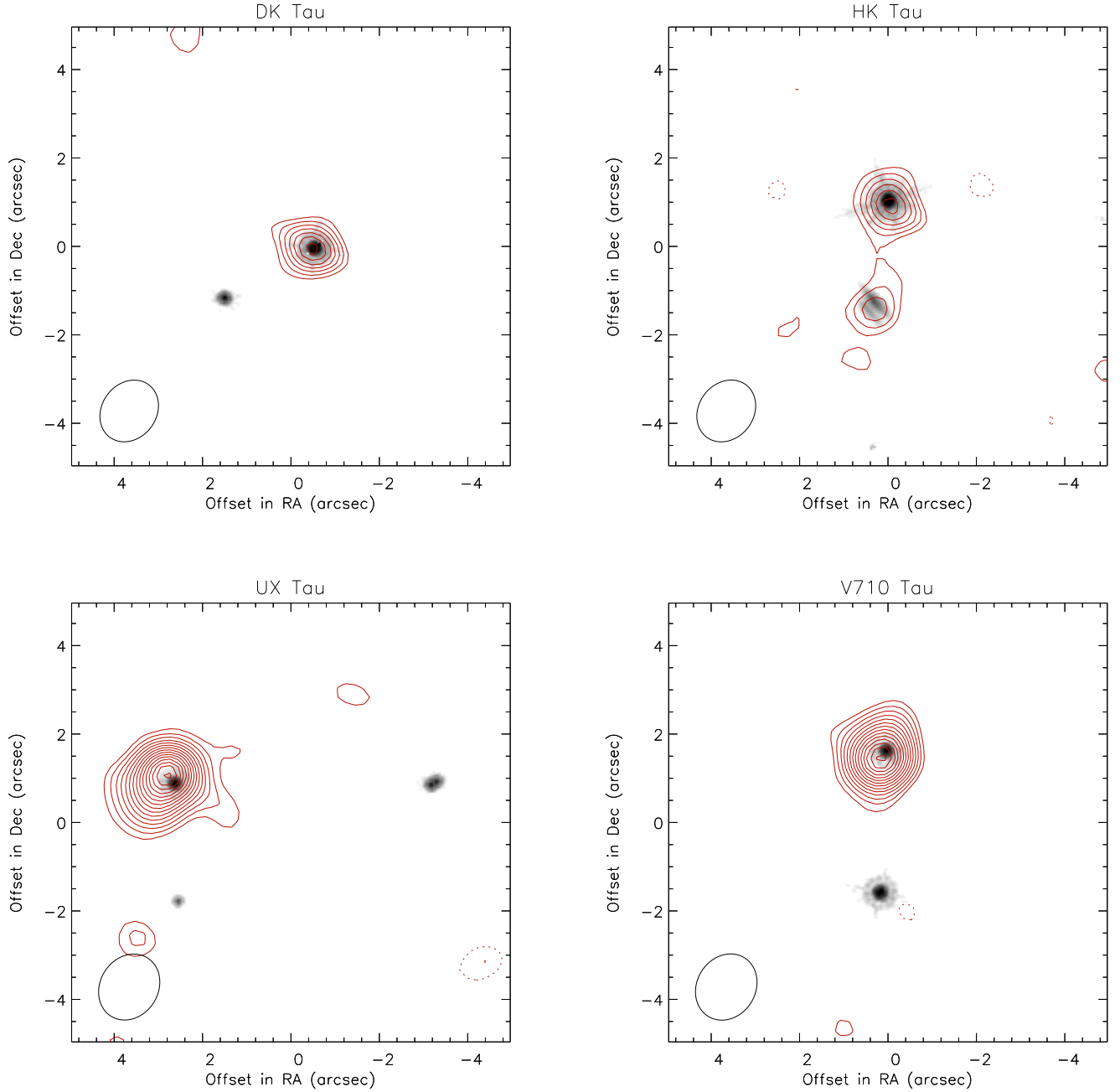


FIG. 1.— Millimeter emission from four young multiple systems. The contours show the $\lambda = 1.3$ mm flux observed with the Owens Valley Millimeter Array overlaid on grayscale optical images from archival Hubble Space Telescope data. In all cases the primary star dominates the disk emission from the system; only in HK Tau, the system with the mass ratio closest to one (see Table 1), is there detectable emission from the secondary. The contours are in steps of the RMS noise in the millimeter maps, 2.1–2.2 mJy, starting at the 3σ contour; negative contours (dashed lines) have the same steps, starting at -3σ . The beam size ($1''.5 \times 1''.3$) is shown at lower left.

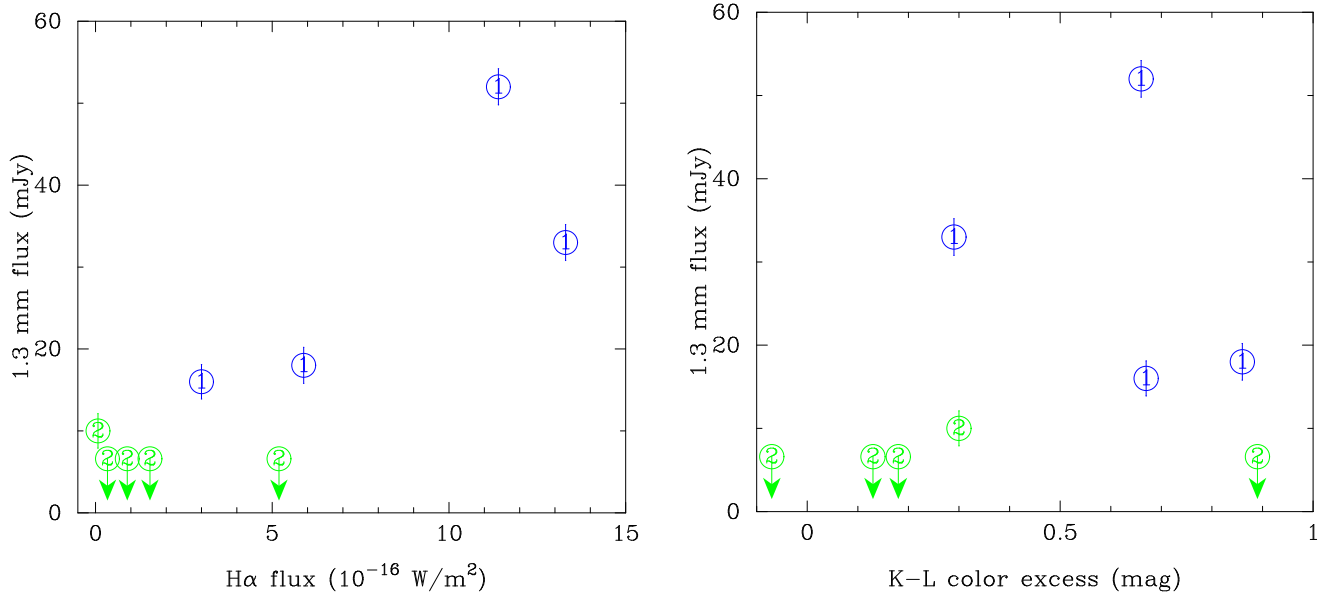


FIG. 2.— Left panel: Millimeter flux vs. H α emission-line flux. Symbols with “1” indicate primary stars, and those with “2” denote secondary or tertiary stars. There is no one-to-one correspondence between H α and mm flux, indicating that disk accretion (traced by H α) is not strongly correlated with disk mass. Right panel: Millimeter flux vs. $K-L$ excess. Again, there is little correlation between $K-L$ excess, a tracer of inner disks, and the overall mass of the disk. H α fluxes are derived from the equivalent widths in Table 1 and continuum fluxes estimated from spectra in Monin, M \acute{e} nard, & Duch \acute{e} ne (1998) or R -band photometry (for V710 Tau only) in Hartigan, Strom, & Strom (1994).

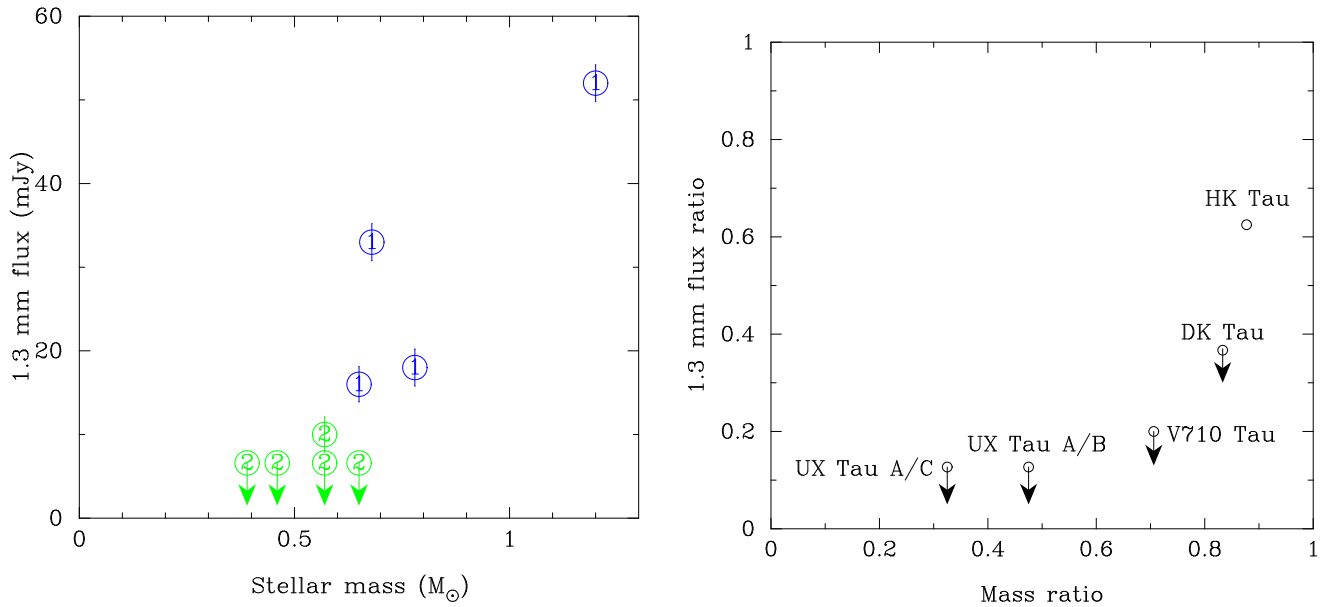


FIG. 3.— Left panel: Millimeter flux vs. stellar mass; symbols are as in Figure 2. There is overlap between the primary and secondary mass distributions, with all primaries being detected while most secondaries, even those with masses comparable to some primaries, are undetected. Right panel: The flux ratio from our millimeter observations vs. the stellar mass ratio. Only when the stellar mass ratio is very close to one is the secondary detected. Both panels suggest that the star’s *relative* mass within the binary system is more important for its disk properties than its absolute mass.

TABLE 1
YOUNG BINARIES OBSERVED

System	Proj. Sep.	Pos. Ang.	Lit. spectral types	Adopted spectral type	H α EW (\AA)	$K-L$	$\Delta(K-L)$	Stellar mass (M_{\odot})	
DK Tau	A		K7–K9	K9	31	0.99 ± 0.04	0.86	0.78	
	B	2''8	115°	K7–M1	M1	118	1.04 ± 0.08	0.89	0.65
HK Tau	A		M1	M1	50	0.82 ± 0.04	0.67	0.65	
	B	2''4	175°	M2	M2	12.5	0.46 ± 0.12	0.30	0.57
UX Tau	A		K2–K5	K4	9.5	0.76 ± 0.06	0.66	1.2	
	B ^a	5''9	269°	M1–M2	M2	4.5	0.09 ± 0.06	–0.07	0.57
	C	2''7	181°	M3–M5	M3	8.5	0.38 ± 0.12	0.18	0.35
V710 Tau	A		M0.5–M1	M0.5	89	0.44 ± 0.04	0.29	0.68	
	B	3''2	177°	M2–M3	M2.5	11	0.31 ± 0.04	0.13	0.48

Note. — Position angle and separation values are from Leinert et al. (1993) and are relative to the primary star. For V710 Tau, component A here is the *optical* primary, though component B (V710 Tau S) is brighter at $2.2 \mu\text{m}$. Adopted spectral types and H α equivalent widths are from Hartigan, Strom, & Strom (1994) for V710 Tau and Duchêne et al. (1999) for all other stars; $K-L$ values are from White & Ghez (2001). Spectral types were used to derive effective temperatures based on Table 2 of Luhman (1999) for the M stars and based on the dwarf temperature scale in Allen (1991) for the K stars. The masses were then estimated from the Baraffe et al. (1998) models assuming an age of 3 Myr, since Luhman (2000) found a sample of young stars in Taurus to lie between the 1 and 3 Myr tracks of the Baraffe et al. (1998) models. Although this method does not produce precise values for the individual masses, the relative masses should be relatively well determined.

^aUX Tau B is a 0''14 binary (Duchêne 1999), unresolved in our data but visible in the HST data in Figure 1.

TABLE 2
MILLIMETER FLUXES

Source		1.3 mm OVRO flux (mJy) ^a	Source size (arcsec) ^b	1.3 mm single-dish flux (mJy) ^c
DK Tau	A	18 ± 2.2	point	35 ± 7
	B	< 6.6	...	
HK Tau	A	16 ± 2.1	point	41 ± 5
	B	14 ± 2.1	point	
UX Tau	A	52 ± 2.2	$1''.1 \times 0''.6$	63 ± 10
	B	< 6.6	...	
	C	< 6.6	...	
V710 Tau	A	33 ± 2.2	point	60 ± 7
	B	< 6.6	...	

^aErrors given are the RMS noise in the maps, and do not include the absolute flux calibration uncertainty of 20%. Upper limits given are 3σ .

^bThe size given for UX Tau A is for a Gaussian fit to the emission. In the fit to HK Tau, there is some diffuse residual emission between the two sources.

^cThe single-dish fluxes are taken from Osterloh & Beckwith (1995) or Beckwith et al. (1990) and have a beam size of $11''$, encompassing all the stars in each system. The uncertainties do not include the absolute flux calibration uncertainty.

TABLE 3
DISK MASS AND RADIUS LOWER LIMITS

Source	Optically thin disk mass ($10^{-3} M_{\odot}$)		Optically thick disk radius (AU)	
	$T = 15$ K	$T = 30$ K		
DK Tau	A	3.4	1.7	9.1
	B	< 1.2	< 0.6	...
HK Tau	A	3.0	1.5	8.4
	B	1.9	0.9	6.1
UX Tau	A	9.7	4.9	18.5
	B	< 1.2	< 0.6	...
	C	< 1.2	< 0.6	...
V710 Tau	A	6.2	3.1	13.6
	B	< 1.2	< 0.6	...